



HAL
open science

A Miniature Tubular Linear Electromagnetic Actuator: Design, Modeling and Experimental Validation

Mouna Ben Salem, Laurent Petit, Muneeb U Khan, Jeremy Terrien, Christine Prella, Frédéric Lamarque, Thibaud Coradin, Christophe Egles

► **To cite this version:**

Mouna Ben Salem, Laurent Petit, Muneeb U Khan, Jeremy Terrien, Christine Prella, et al.. A Miniature Tubular Linear Electromagnetic Actuator: Design, Modeling and Experimental Validation. International Conference on Manipulation, Automation and Robotics at Small Scales (MARSS), Jul 2022, Toronto, Canada. 10.1109/MARSS55884.2022.9870253 . hal-03837852

HAL Id: hal-03837852

<https://hal.science/hal-03837852>

Submitted on 3 Nov 2022

HAL is a multi-disciplinary open access archive for the deposit and dissemination of scientific research documents, whether they are published or not. The documents may come from teaching and research institutions in France or abroad, or from public or private research centers.

L'archive ouverte pluridisciplinaire **HAL**, est destinée au dépôt et à la diffusion de documents scientifiques de niveau recherche, publiés ou non, émanant des établissements d'enseignement et de recherche français ou étrangers, des laboratoires publics ou privés.

A Miniature Tubular Linear Electromagnetic Actuator: Design, Modeling and Experimental Validation

Mouna Ben Salem¹, Laurent Petit¹, Muneeb Ullah Khan¹, Jeremy Terrien², Christine Prelle¹, Frédéric Lamarque¹, Thibaud Coradin³, Christophe Egles⁴

Abstract—In this paper, a miniature tubular linear actuator capable of moving and reaching discrete positions inside a tube is presented. Its small size and ability to realize small strokes makes it suitable for biomedical applications. We then present the electromagnetic modeling of the actuator followed by an experimental validation. Results show that the actuator can reach discrete positions inside the tube with an average value of 3.5 mm and a standard deviation of 0.1 mm for a supplied current of 0.5 A.

I. INTRODUCTION

Tubular linear actuators have been widely used in different applications owing to the fact that they can offer several advantages compared to rotary systems such as high precision, higher dynamic performance and enhanced reliability [1]. They are often used in industrial applications where fast response and accurate movements in tight places are needed with high-precision such as in manufacturing automation [2], Pick-and-Place robots [3] and piping inspection robots [4]. At a smaller scale, tubular actuators are also used in biomedical applications that require movement within the human body such as wireless active enteroscopy recently developed in [5], laparoendoscopic single-site surgery [6] and inchworm movement which is often used in robots passing through highly constrained places such as the human gastrointestinal tract [7], [8].

Several architectures and physical principles have been explored by research teams to develop tubular linear actuators. Many electromagnetic actuators are described in literature [3], [5], [9]. Some research studies focused on designing the moving-magnet linear actuator with cylindrical Halbach array [10], others focused on tubular actuators with the levitation function [9], [11]. Inchworm-type piezoelectric linear actuator has also been studied and characterized [12]. Applications for this type of actuator include smart or adaptive structural systems in auto and aerospace industries. Several studies that focus on muscle-like actuators also

known as dielectric elastomers have been presented, they can sustain large deformation, have a high energy density and a relatively fast response [13]. As an example, a compact dielectric elastomer tubular actuator used for a refreshable full page Braille display is presented in [14]. Moreover, tubular shape memory alloy actuator are described in [15]. It is used for active catheters that will enhance research for precise miniature instruments to achieve accurate positioning for complex and minimally invasive surgical procedures. Linear actuators have also played a very important role in the development and progress in the domain of soft robots [16], [17]. For example, dielectric elastomer linear actuators, thermoresponsive linear actuators and linear actuators driven by ionic diffusion or pressurized fluidics are developed for soft robots [18].

In this paper, we propose a miniature tubular electromagnetic actuator that can reach discrete positions inside a tube. It can be used in a biomedical application where an action is done periodically such as substance delivery. Therefore, an actuator with several discrete positions is developed which represents an originality for this type of application. In section II, the tubular actuator, its working principle as well as the geometrical and magnetic parameters are presented. Section III is dedicated to the electromagnetic modeling of the actuator in order to determine the generated force on the mobile part. Based on this modeling, a prototype was developed for which an experimental characterization is presented in section IV. Finally, the conclusion and perspectives of this work are presented in section V.

II. WORKING PRINCIPLE

The tubular linear actuator is based on an electromagnetic actuation principle [19]. As shown in Fig. 1a, the actuator consists of a Permanent Magnet (PM), with axial magnetization, placed inside a tube. For now, there is only mechanical contact between the PM and the tube. In the future, the actuator environment will have fluid to take into consideration. To achieve desired dimensions, a pair of 3 mm long PMs are used. The geometrical and magnetic parameters of the components are illustrated in Fig. 1b and their values are provided in table - I.

The PM is placed, and freely moving, inside the tube around which coils are assembled. To reach discrete positions inside the tube, four coils are used. When the coils are injected with current, the generated electromagnetic field enables the PM to move forward or backward in order to reach discrete positions inside the tube. To validate the

*This work is supported by The Initiative MSTD (Maîtrise des Systèmes Technologiques sûrs et Durables)

¹Mouna Ben Salem, Laurent Petit, Muneeb Ullah Khan, Christine Prelle and Frédéric Lamarque are with Roberval Laboratory (Mechanics, Energy and Electricity), Université de Technologie de Compiègne, 60200 Compiègne, France. mouna.ben-salem@utc.fr

²Jeremy Terrien is with the Department of Electronics, Sorbonne Université, Université de Technologie de Compiègne, 60200 Compiègne, France.

³Thibaud Coradin is with Sorbonne Université, CNRS, Laboratory of Chemistry of Condensed Matter of Paris, 75005 Paris, France

⁴Christophe Egles is with Université de Technologie de Compiègne, CNRS, UMR 7338 Biomechanics and Bioengineering (BMBI), 60203 Compiègne, France.

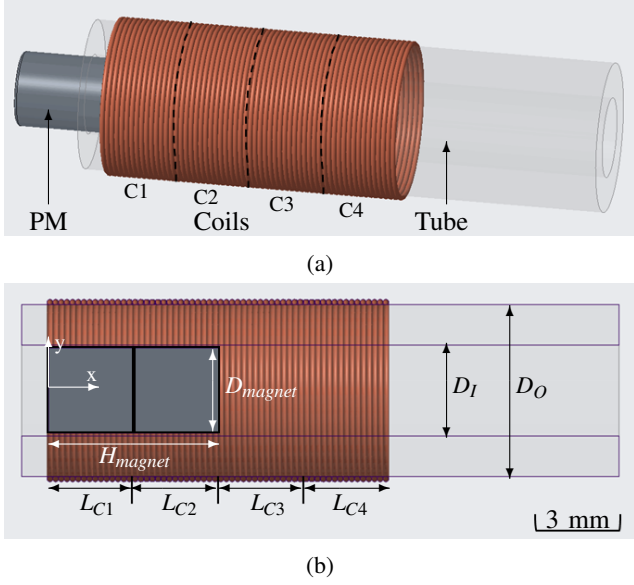


Fig. 1: Schematic layout of the actuator: (a) design and main components, (b) geometrical parameters.

TABLE I: Physical parameters of the tubular actuator.

Variable	Value
Permanent Magnet	
Diameter D_{magnet}	3 mm
Height H_{magnet}	3 mm
Magnetic flux density	1.17 T
Material	NdFeB
Mass	154.5 mg
Coils	
Wire diameter	0.2 mm
Length $L_{C1}, L_{C2}, L_{C3}, L_{C4}$	3 mm
Segment number	15
Material	Copper
Tube	
Inside diameter D_I	3.2 mm
Outside diameter D_O	6 mm
Length	150 mm
Material	Clear acrylic

working principle of the actuator, an electromagnetic model has been developed and is detailed in the following section.

III. ELECTROMAGNETIC MODELING

In order to carry out the electromagnetic modeling of the actuator, we used a semi-analytical software RADIA which is a Mathematica addon developed by The European Synchrotron Radiation Facility (ESRF). As shown in Fig 2, we have modeled the PM with a cylindrical element having dimensions and magnetization given in table-I. The coils are also modeled side by side with the previously identified dimensions.

The electromagnetic force exerted by each coil on the PM, when they are supplied with a current of 1 A, were calculated for the position of the PM with a calculation step of 1 mm. It should be noted that the presented position corresponds to the center of the PM.

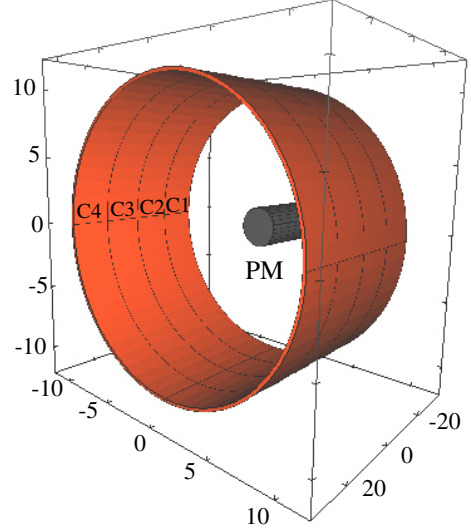


Fig. 2: 3D model of an actuator in RADIA software.

The results of the electromagnetic simulation are presented in Fig 3. The maximum forces generated by the coils (± 3.2 mN) are shifted apart 3 mm which makes sense because it corresponds to the length of a coil.

When the PM is centered to the coil (i.e., $L_{C1}/2, L_{C2}/2$, etc.), the force is zero. However, the effort is maximum (positive or negative) when the PM is placed close to the face of a coil. Therefore, this architecture allows to successively move the PM from one position to the next one supplying one coil then the next one.

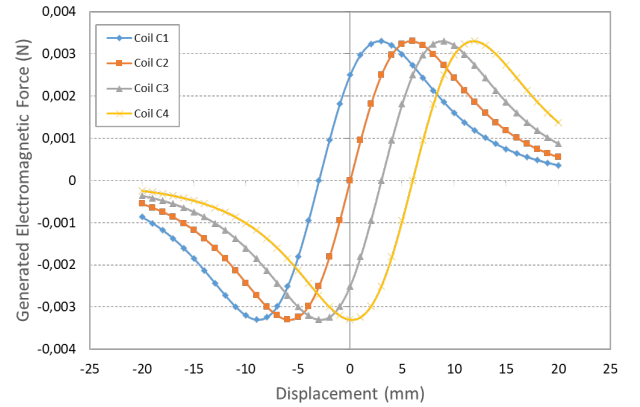
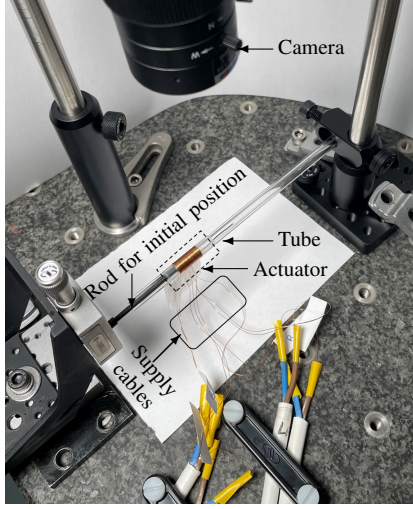


Fig. 3: Simulation results of the electromagnetic modeling.

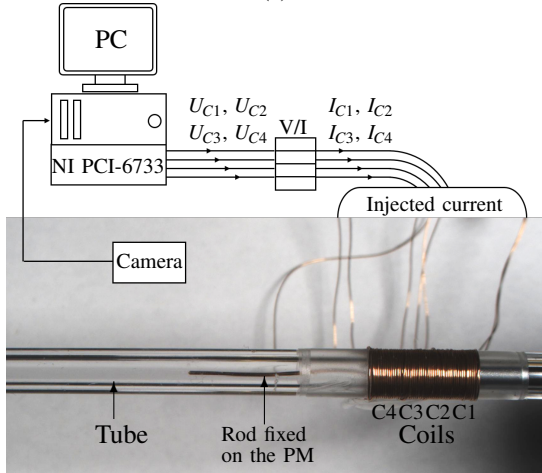
IV. EXPERIMENTAL SETUP AND RESULTS

To carry out the experimental validation of the actuator, a prototype has been built (see Fig. 4). In addition, to measure the displacement realized by the pair of PM, a camera is used to take pictures of the rod that has a mass of 60 mg and is assembled on the PM as illustrated in Fig. 4c. The initial position is set with the help of the rod fixed on a linear stage (as shown in Fig. 4a). The objective of this initial positioning of PM inside the tube is necessary to deliver maximum force.

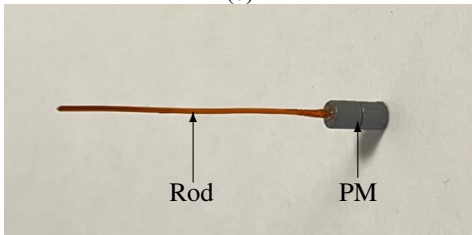
Therefore, the PM is positioned in such a way that its lower face coincides with the start of the coil C1. Since it is 6 mm long, it will be completely surrounded by the first two coils C1 and C2.



(a)



(b)



(c)

Fig. 4: Experimental validation: (a) dedicated setup, (b) prototype of the tubular linear actuator, (c) PM and rod used.

In order to inject desired currents in coils, a program is set up through the LabVIEW interface (National Instruments CorporationTM). We used the I/O board NI PCI-6733 along with 4 Voltage to Current (V/I) converters (input = ± 10 V, output = ± 10 A, bandwidth of 50 kHz). To measure the PM position, a high resolution camera (Grasshopper3 GS3-U3-32S4C) has been used and placed above the prototype.

With the camera, pictures are taken and the PM position is then determined considering the pixel size which has been determined thanks to a calibration (1 pixel = $40 \mu\text{m}$).

A. Single coil characterization

First, we started by supplying only the first coil C1 with a current ranging from 0 A to 1 A, with a step of 0.1 A in order to calculate the displacement of the PM according to the current amplitude. The results of this first measurement are shown in Fig. 5. The measurements were repeated 5 times to calculate the error and the dispersion (standard deviation) on the displacement values.

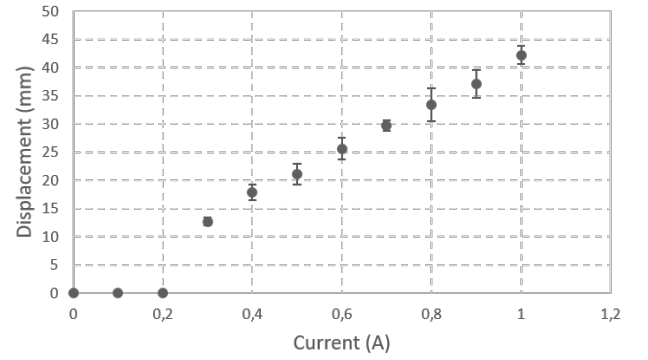


Fig. 5: Influence of the current on the PM displacement for a single coil C1.

From the obtained results shown in Fig. 5, it can be observed that the PM moves forward inside the tube for a current value starting from 0.3 A with a minimum displacement of 12.7 mm and a maximum displacement of 42.2 mm obtained with a 1 A current with a standard deviation of 0.6 mm and 1.5 mm, respectively. Below 0.3 A, the current is not sufficient to allow the displacement of the PM because of the friction present inside the tube. The friction coefficient is determined with an inclined plane technique and is found to be 0.65 ± 0.03 . We observe that by supplying current to one coil, we are able to move the PM inside the tube. However, the displacement obtained is high. Smaller displacements could be reached in a controlled manner by supplying two coils with opposite currents in order to reach a stable position.

B. Characterization of a coil pair

Here, we supplied the first two coils C1 and C2 with several combinations of opposite currents varying from 0 A to 1 A with a step of 0.1 A as shown in table - II. When the positive-supplied coil pushes the PM forward, the negative-supplied coil pulls it back creating a stable position. The results of this measurement along with the repeatability error are illustrated in Fig. 6. The measurements were repeated 5 times to calculate the error and the dispersion (standard deviation) on the displacement values.

The results show that the displacement of the PM is ensured starting from a current amplitude of +0.2 A in C1 and -0.2 A in C2. The displacement varies from $3.4 \text{ mm} \pm 0.1 \text{ mm}$

TABLE II: Combinations of controlling currents.

Combination	Current C1 (A)	Current C2 (A)	Displacement (mm)
0	0	0	0
1	0.1	-0.1	0
2	0.2	-0.2	4.4 ± 0.1
3	0.3	-0.3	3.4 ± 0.1
4	0.4	-0.4	3.9 ± 0.2
5	0.5	-0.5	3.9 ± 0.2
6	0.6	-0.6	3.5 ± 0.1
7	0.7	-0.7	3.7 ± 0.1
8	0.8	-0.8	3.5 ± 0.09
9	0.9	-0.9	3.7 ± 0.1
10	1	-1	3.8 ± 0.1

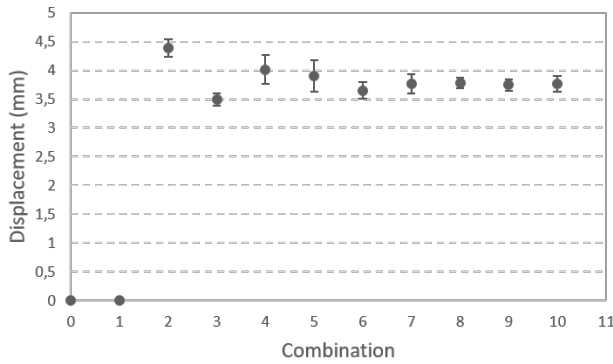


Fig. 6: Characterization of the PM displacement for a coil pair.

to $4.4 \text{ mm} \pm 0.1 \text{ mm}$ with an average value of 3.8 mm . Therefore, it is not necessary to use high amplitude currents. By combining two coils supplied with opposite currents, a displacement step of the PM can be obtained which makes it possible to achieve our objective to realize periodic displacement strokes, by moving the PM towards defined positions inside the tube.

C. Multi-positions characterization

The third presented measurement consists of supplying the coils two by two to drive the PM inside the tube between several positions to measure the ones reached with the 4 coils. Based on the results of the previous measurement, we chose to use a current amplitude of 0.5 A which is located in the middle of the range studied in Fig. 6. The results of this measurement as well as the repeatability error are shown in Fig. 7. The measurements were repeated 5 times to calculate the error and the dispersion (standard deviation) on the displacement values.

Initially, the PM is at its initial position as shown in Fig. 8a. First, coils C1 and C2 are supplied with a current of 0.5 A and -0.5 A , respectively. The PM moves over a distance of $3.8 \text{ mm} \pm 0.1 \text{ mm}$ (see Fig. 8b). Then, coils C2 and C3 are supplied with a current of 0.5 A and -0.5 A , respectively moving the PM to a position of $7.1 \text{ mm} \pm 0.1 \text{ mm}$ i.e., a displacement of $3.3 \text{ mm} \pm 0.1 \text{ mm}$ (see Fig. 8c). Finally, coils C3 and C4 are supplied with a current of 0.5 A and

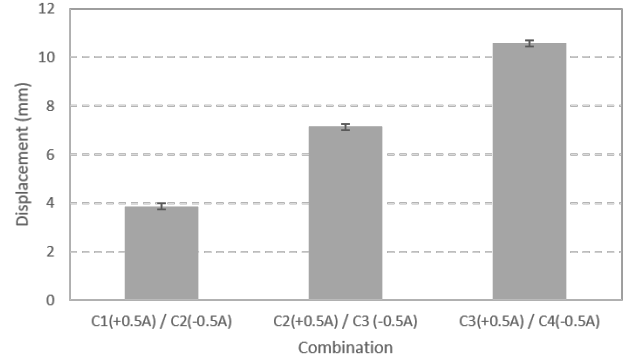


Fig. 7: Multi-positions characterization.

-0.5 A , respectively which ensures a PM displacement to a position of $10.5 \text{ mm} \pm 0.1 \text{ mm}$ i.e., a displacement of $3.4 \text{ mm} \pm 0.2 \text{ mm}$ (see Fig. 8d).

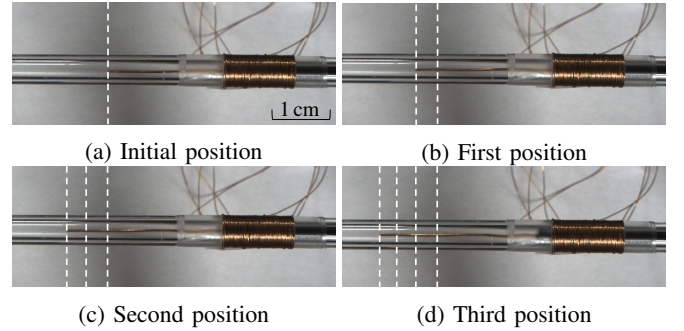


Fig. 8: Positions reached by the tubular actuator.

We observe a slight difference between the positions reached by the PM. This problem is due to the assembly errors (especially that of the coils). Despite these error, the objective of this work is to validate the working principle. In future, a more optimized version addressing all these problems will be designed to achieve better performances.

V. CONCLUSIONS AND PERSPECTIVES

In this paper, we proposed a tubular linear electromagnetic actuator which aims to reach discrete positions inside a tube. First, we presented the actuator architecture and an electromagnetic modeling to compute the electromagnetic force generated by each coil according to the position of the PM inside the tube. The results show that each coil could generate a maximum force of 3.2 mN with a supplied current of 1 A .

Afterwards, a prototype and a setup were built for experimental validation. First, the PM displacement has been measured by supplying one single coil. It was observed that the PM motion is not obtained with a supplied current lower than 0.3 A due to friction. With a current higher to this value, the PM displacement increases linearly and reaches $42.2 \text{ mm} \pm 1.5 \text{ mm}$ with 1 A . A second measurement was made by supplying two coils simultaneously with equal and opposite currents in order to reach discrete positions

inside the tube. It was observed that the PM moves with an average value step of 3.8 mm. Finally, the ability of the PM to reach several positions inside the tube when supplying the couple of coils has been characterized. With four coils, it was observed that the PM is able to reach three positions located at $3.8 \text{ mm} \pm 0.1 \text{ mm}$, $7.1 \text{ mm} \pm 0.1 \text{ mm}$ and $10.5 \text{ mm} \pm 0.1 \text{ mm}$.

Future work will focus mainly on the design modification of the actuator and its optimization. Generally, elements can be added to index the positions that the PM can reach in order to improve the performance obtained. This indexing will reduce the difference observed between the PM steps but also reduce the repeatability error. For example, this could be done magnetically by ferromagnetic rings distributed evenly along the tube. Future work will also consist in developing a dynamic model to estimate the displacement of the PM and compare the results with the experimental displacements in order to validate the theoretical approach. In the longer term, the integration of this type of actuator for biomedical applications will be considered.

REFERENCES

- [1] L. Encica, J. J. H. Paulides, E. A. Lomonova, and A. J. A. Vandenput, "Electromagnetic and Thermal Design of a Linear Actuator Using Output Polynomial Space Mapping," *IEEE Transactions on Industry Applications*, vol. 44, no. 2, pp. 534–542, 2008.
- [2] Z. Zhang and H. Liu, "A Novel Force Ripple Reduction Method of Tubular Linear Switched Reluctance Actuators based on Multi-stages Translator Poles," in *International Symposium on Linear Drives for Industry Applications*, 2021, pp. 1–4.
- [3] K. J. Meessen, J. J. H. Paulides, and E. A. Lomonova, "Modeling and experimental verification of a tubular actuator for 20 g acceleration in a pick and place application," in *IEEE International Electric Machines and Drives Conference*, 2009, pp. 419–424.
- [4] D. Chablat, S. Venkateswaran, and F. Boyer, "Mechanical design optimization of a piping inspection robot," *Procedia Cirp*, vol. 70, pp. 307–312, 2018.
- [5] H. Khan and A. Cuschieri, "Low powered Uni-directional actuator for wireless active enteroscopy," in *ACTUATOR ; International Conference and Exhibition on New Actuator Systems and Applications*, 2021, pp. 1–4.
- [6] W. Yue, R. Tang, J. S. Wong, and H. Ren, "Deployable tubular mechanisms integrated with magnetic anchoring and guidance system," in *Actuators*, vol. 11, no. 5, 2022, p. 124.
- [7] J. Zhu, H. Lu, Y. Guo, and Z. Lin, "Development of electromagnetic linear actuators for micro robots," in *International Conference on Electrical Machines and Systems*, 2008, pp. 3673–3679.
- [8] L. Phee, D. Accoto, A. Menciassi, C. Stefanini, M. C. Carrozza, and P. Dario, "Analysis and development of locomotion devices for the gastrointestinal tract," *IEEE Transactions on Biomedical Engineering*, vol. 49, no. 6, pp. 613–616, 2002.
- [9] C. Weißbacher, H. Stelzer, and K. Hameyer, "Application of a Tubular Linear Actuator as an Axial Magnetic Bearing," *IEEE/ASME Transactions on Mechatronics*, vol. 15, no. 4, pp. 615–622, 2010.
- [10] S.-M. Jang, J.-Y. Choi, H.-W. Cho, and S.-H. Lee, "Thrust analysis and measurements of tubular linear actuator with cylindrical halbach array," *IEEE Transactions on Magnetics*, vol. 41, no. 5, pp. 2028–2031, 2005.
- [11] S. Mirić, P. Küttel, A. Tüysüz, and J. Kolar, "Design and Experimental Analysis of a New Magnetically Levitated Tubular Linear Actuator," *IEEE Transactions on Industrial Electronics*, 2019.
- [12] J. Li, R. Sedaghati, J. Dargahi, and D. Waechter, "Design and development of a new piezoelectric linear Inchworm® Inchworm is a registered trademark of Burleigh Instruments Inc.® actuator," *Mechatronics*, vol. 6, no. 15, pp. 651–681, 2005.
- [13] R. Sarban, R. Jones, B. Mace, and E. Rustighi, "A tubular dielectric elastomer actuator : Fabrication, characterization and active vibration isolation," *Mechanical Systems and Signal Processing - MECH SYST SIGNAL PROCESS*, vol. 25, pp. 2879–2891, 2011.
- [14] P. Chakraborti, H. A. K. Toprakci, P. Yang, N. Di Spigna, P. Franzon, and T. Ghosh, "A compact dielectric elastomer tubular actuator for refreshable Braille displays," *Sensors and Actuators A : Physical*, vol. 179, pp. 151–157, 2012.
- [15] A. Tung, B.-H. Park, A. Koolwal, B. Nelson, G. Niemeyer, and D. Liang, "Design and Fabrication of Tubular Shape Memory Alloy Actuators for Active Catheters," in *The First IEEE/RAS-EMBS International Conference on Biomedical Robotics and Biomechanics, 2006. BioRob 2006.*, 2006, pp. 775–780.
- [16] N. El-Atab, R. B. Mishra, F. Al-Modaf, L. Joharji, A. A. Alsharif, H. Alamoudi, M. Diaz, N. Qaiser, and M. M. Hussain, "Soft actuators for soft robotic applications : a review," *Advanced Intelligent Systems*, vol. 2, no. 10, p. 2000128, 2020.
- [17] P. Boyraz, G. Runge, and A. Raatz, "An overview of novel actuators for soft robotics," in *Actuators*, vol. 7, no. 3, 2018, p. 48.
- [18] X. Cao, M. Zhang, Z. Zhang, Y. Xu, Y. Xiao, and T. Li, "Review of soft linear actuator and the design of a dielectric elastomer linear actuator," *Acta Mechanica Solida Sinica*, vol. 32, no. 5, pp. 566–579, 2019.
- [19] N. Arora, M. U. Khan, L. Petit, F. Lamarque, and C. Prella, "Design and development of a planar electromagnetic conveyor for the micro-factory," *IEEE/ASME Transactions on Mechatronics*, vol. 24, no. 4, pp. 1723–1731, 2019.